Optimized Overlapping DDFV Schwarz Algorithms

Martin J. Gander[1], Laurence Halpern[2], Florence Hubert[3], and Stella Krell[4]

1 Introduction

We are interested in parallel solvers for the anisotropic diffusion problem

$$\mathcal{L}(u) := -\mathrm{div}(A\nabla u) + \eta u = f \text{ in } \Omega, \quad u = 0 \quad \text{on } \partial\Omega, \tag{1}$$

$$\text{with } (x,y) \in \Omega \mapsto A(x,y) = \begin{pmatrix} A_{xx} & A_{xy} \\ A_{xy} & A_{yy} \end{pmatrix}, \quad \eta > 0, \tag{2}$$

where A is a uniformly symmetric positive definite matrix. Non-overlapping optimized Schwarz methods have been developed for (1) discretized with Discrete Duality Finite Volume (DDFV) schemes [6], because these techniques are especially well suited for anisotropic diffusion [7], [3], [1]. Since overlap in general greatly enhances the performance of Schwarz algorithms, we introduce and test here a new, optimized overlapping DDFV Schwarz algorithm, and we show that a discrete and bounded domain convergence analysis is important to get best performance for strong anisotropy.

2 Optimized overlapping Schwarz algorithm

For simplicity, we describe the algorithm for two rectangular subdomains with overlap, $\Omega = \Omega_1 \cup \Omega_2$, $\Omega_1 \cap \Omega_2 \neq \emptyset$, with interfaces $\Gamma_j = \partial\Omega_j \setminus \partial\Omega_j \cap \partial\Omega$, see Figure 1. A general parallel[1] Schwarz method on these two subdomains

University of Geneva, 2-4 rue du Lièvre, CP 64, 1211 Genève, Switzerland, martin.gander@unige.ch · Université PARIS 13, LAGA, 93430 Villetaneuse, FRANCE, halpern@math.univ-paris13.fr · Aix-Marseille Université, CNRS, Centrale Marseille, I2M UMR 7373, 39 rue F. Joliot Curie, 13453 Marseille, Cedex 13, FRANCE, florence.hubert@univ-amu.fr · Université de Nice, Parc Valrose, 28 avenue Valrose, 06108 Nice, Cedex 2, FRANCE, krell@unice.fr

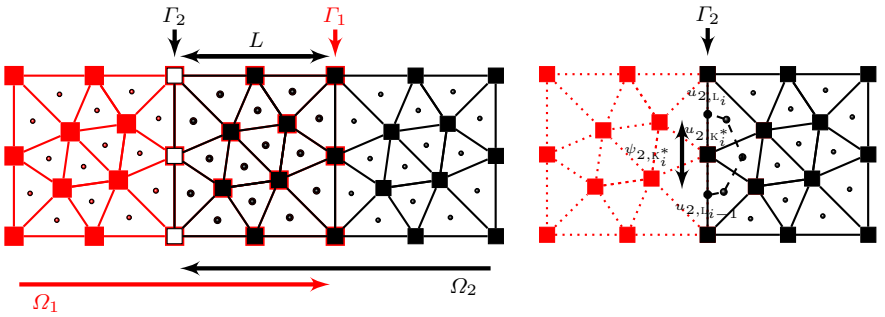

Fig. 1 Left: example of overlapping meshes, primal meshes $\mathfrak{M}_j$ are shown. Right: detailed notation near the interface Γ_2.

is given by solving for $n = 1, 2, \ldots$ the subdomain problems

$$\mathcal{L}u_j^n = f \text{ in } \Omega_j, \quad u_j^n = 0 \text{ on } \partial\Omega_j \cap \partial\Omega,$$
$$\mathcal{B}_1 u_1^n = \mathcal{B}_1 u_2^{n-1} \text{ on } \Gamma_1, \quad \mathcal{B}_2 u_2^n = \mathcal{B}_2 u_1^{n-1} \text{ on } \Gamma_2.$$

If we choose for the transmission operators $\mathcal{B}_j$ the identity, we obtain the classical Schwarz method. If we choose $\mathcal{B}_j := A_{xx}\partial_{n_j} + P(\partial_y)$ with $P(\partial_y) = p - qA_{yy}\partial_{yy}$, we obtain the so called optimized Schwarz methods [4], with Robin ($q = 0$) or Ventcell ($q \neq 0$) transmission conditions and overlap L,

$$\begin{aligned} A_{xx}\partial_x u_1^n(L, y) + Pu_1^n(L, y) &= A_{xx}\partial_x u_2^{n-1}(L, y) + Pu_2^{n-1}(L, y), \\ -A_{xx}\partial_x u_2^n\ (0, y) + Pu_2^n(0, y) &= -A_{xx}\partial_x u_1^{n-1}(0, y) + Pu_1^{n-1}(0, y). \end{aligned} \tag{3}$$

The convergence, discretization and optimization of such algorithms in the nonoverlapping case were studied in [6]; we study here for the first time the overlapping case.

3 DDFV Discretization

We now describe the DDFV Schwarz algorithm for overlapping subdomains and decompositions using the notation from [2], see Fig. 2.

The meshes: for $j = 1, 2$, the primal mesh $\mathfrak{M}_j$ is a set of disjoint open polygonal control volumes $\kappa \subset \Omega_j$ such that $\cup\overline{\kappa} = \overline{\Omega_j}$. We denote by $\partial\mathfrak{M}_j$ the set of edges of the control volumes in $\mathfrak{M}_j$ included in $\partial\Omega_j$, and by $\partial\mathfrak{M}_{\Gamma_j}$ the subset of $\partial\Omega_j$ of edges of primal boundary cells related to the interface $\Gamma_j = \partial\Omega_j \cap \Omega_i$ (*i.e.* in what follows, $i = 2$ if $j = 1$, and $i = 1$ if $j = 2$). We assume that each edge of Γ_j corresponds to an edge of $\mathfrak{M}_i$. We use

[1] or alternating if $\mathcal{B}_2 u_1^n$ is transmitted on Γ_2, leaving the rest unchanged

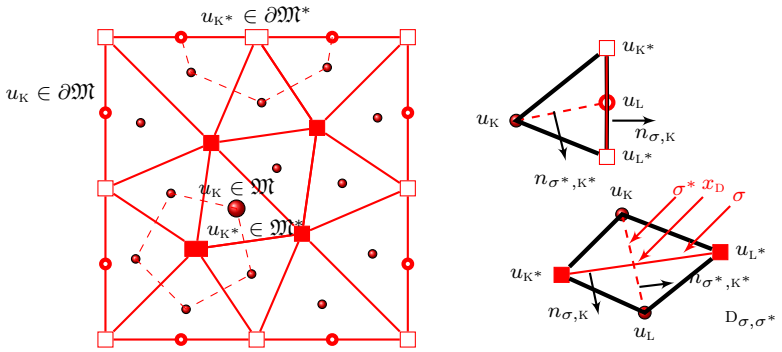

Fig. 2 Left: primal mesh and some dual cells. Right: diamond cell D_{σ,σ^*}.

the same notation for the dual mesh, $\mathfrak{M}_j^*$, $\partial\mathfrak{M}_j^*$ and $\partial\mathfrak{M}_{\Gamma_j}^*$. We define the diamond cells D_{σ,σ^*} as the quadrangles whose diagonals are a primal edge $\sigma = K|L = (x_{K^*}, x_{L^*})$ and a corresponding dual edge $\sigma^* = K^*|L^* = (x_K, x_L)$. The set of diamond cells is called the diamond mesh, denoted by $\mathfrak{D}_j$.

For any V in $\mathfrak{M}_j \cup \partial\mathfrak{M}_j$ or $\mathfrak{M}_j^* \cup \partial\mathfrak{M}_j^*$, we denote by m_V its Lebesgue measure, by $\mathcal{E}_V$ the set of its edges, and $\widetilde{\mathfrak{D}}_V := \{D_{\sigma,\sigma^*} \in \mathfrak{D}_j,\ \sigma \in \mathcal{E}_V\}$. For $D = D_{\sigma,\sigma^*}$ with vertices $(x_K, x_{K^*}, x_L, x_{L^*})$, we denote by x_D the center of D, that is the intersection of the primal edge σ and the dual edge σ^*, by m_D its measure, by m_σ the length of σ, by m_{σ^*} the length of σ^*, by $m_{\sigma_{K^*}}$ the length of $\partial K^* \cap \Omega_j$, by m_{σ_L} the length of $D \cap \partial\Omega_j$, and by m_{σ_K} the length of $[x_K, x_D]$. $\mathbf{n}_{\sigma K}$ is the unit vector normal to σ oriented from x_K to x_L, and $\mathbf{n}_{\sigma^* K^*}$ is the unit vector normal to σ^* oriented from x_{K^*} to x_{L^*}.

For $\sigma = \partial\mathfrak{M}_{\Gamma_j}$, there exists $\widetilde{D} \in \mathfrak{D}_i$ whose vertices are $x_{K_i}, x_{K^*}, x_L, x_{L^*}$ with $x_{K_i} \in \Omega_i$. We denote by the half-diamond D_i the triangle whose vertices are $x_{K_i}, x_{K^*}, x_{L^*}$ and by the half-diamond D_j the triangle whose vertices are $x_{K_j}, x_{K^*}, x_{L^*}$, where $K_j \in \mathfrak{M}_j$ such that $\sigma \in \partial K_j$. Then let $D = D_i \cup D_j$ and $\mathfrak{D}_{\Gamma_j}$ be the set of these diamonds.

The unknowns: the DDFV method associates to all primal control volumes $K \in \mathfrak{M}_j \cup \partial\mathfrak{M}_j$ an unknown value $u_{j,K}$, and to all dual control volumes $K^* \in \mathfrak{M}_j^* \cup \partial\mathfrak{M}_j^*$ an unknown value u_{j,K^*}. To handle the transmission condition on Γ_j, we also require a flux unknown ψ_{j,K^*} per boundary dual cell $K \in \partial\mathfrak{M}_{\Gamma_j}^*$. We denote the approximate solution on the mesh $\mathcal{T}_j$ by $u_{\mathcal{T}_j} = ((u_{j,K})_{K\in(\mathfrak{M}_j\cup\partial\mathfrak{M}_j)}, (u_{j,K^*})_{K^*\in(\mathfrak{M}_j^*\cup\partial\mathfrak{M}_j^*)}, (\psi_{j,K^*})_{K^*\in\partial\mathfrak{M}_{\Gamma_j}^*}) \in \mathbb{R}^{\mathcal{T}_j}$. When f is a continuous function, we define for all control volumes $C \in \mathcal{T}_j$, $f_{\mathcal{T}_j} = (f_C)$ by $f_C := f(x_C)$.

Operators. DDFV schemes can be described by two operators: a discrete gradient $\nabla^{\mathfrak{D}_j}$ and a discrete divergence $\mathrm{div}^{\mathcal{T}_j}$, which are dual to each other, see [2]. Let $\nabla^{\mathfrak{D}_j} : u_{\mathcal{T}_j} \in \mathbb{R}^{\mathcal{T}_j} \mapsto \left(\nabla^D u_{\mathcal{T}_j}\right)_{D\in\mathfrak{D}_j} \in (\mathbb{R}^2)^{\mathfrak{D}_j}$ and $\mathrm{div}^{\mathcal{T}_j} : \xi_{\mathfrak{D}_j} = (\xi_D)_{D\in\mathfrak{D}_j} \mapsto \mathrm{div}^{\mathcal{T}_j}\xi_{\mathfrak{D}_j} \in \mathbb{R}^{\mathcal{T}_j}$ be defined as

$$\nabla^{\mathrm{D}} u_{\mathcal{T}_j} := \frac{1}{2m_{\mathrm{D}}}\left((u_{\mathrm{L}}-u_{\mathrm{K}})m_\sigma \mathbf{n}_{\sigma\mathrm{K}} + (u_{\mathrm{L}^*}-u_{\mathrm{K}^*})m_{\sigma^*}\mathbf{n}_{\sigma^*\mathrm{K}^*}\right), \quad \forall \mathrm{D}\in\mathfrak{D}_j,$$

$$\mathrm{div}^{\mathrm{K}}\xi_{\mathfrak{D}_j} := \frac{1}{m_{\mathrm{K}}}\sum_{\mathrm{D}\in\mathfrak{D}_{\mathrm{K}}} m_\sigma(\xi_{\mathrm{D}},\mathbf{n}_{\sigma\mathrm{K}}),\ \forall \mathrm{K}\in\mathfrak{M}_j, \text{ and } \mathrm{div}^{\mathrm{K}}\xi_{\mathfrak{D}_j}=0, \forall \mathrm{K}\in\partial\mathfrak{M}_j,$$

$$\mathrm{div}^{\mathrm{K}^*}\xi_{\mathfrak{D}_j} := \frac{1}{m_{\mathrm{K}^*}}\sum_{\mathrm{D}\in\mathfrak{D}_{\mathrm{K}^*}} m_{\sigma^*}(\xi_{\mathrm{D}},\mathbf{n}_{\sigma^*\mathrm{K}^*}),\ \forall \mathrm{K}^*\in\mathfrak{M}_j^*\cup\partial\mathfrak{M}_j^*.$$

DDFV scheme on Ω_j for Ventcell boundary conditions on Γ_j.

For $u_{\mathcal{T}_j}\in\mathbb{R}^{\mathcal{T}_j}$, $f_{\mathcal{T}_j}\in\mathbb{R}^{\mathcal{T}_j}$ and $h_{\mathcal{T}_j}\in\mathbb{R}^{\partial\mathfrak{M}_{\Gamma_j}\cup\partial\mathfrak{M}^*_{\Gamma_j}}$, we denote by $\mathcal{L}^{\mathcal{T}_j}_{\Omega_j}(u_{\mathcal{T}_j},f_{\mathcal{T}_j},h_{\mathcal{T}_j})=0$ the linear system

$$-\mathrm{div}^{\mathrm{K}}\left(A_{\mathfrak{D}}\nabla^{\mathfrak{D}}u_{\mathcal{T}_j}\right)+\eta_{\mathrm{K}}u_{j,\mathrm{K}}=f_{\mathrm{K}},\quad \forall\ \mathrm{K}\in\mathfrak{M}_j, \tag{4}$$

$$-\mathrm{div}^{\mathrm{K}^*}\left(A_{\mathfrak{D}}\nabla^{\mathfrak{D}}u_{\mathcal{T}_j}\right)+\eta_{\mathrm{K}^*}u_{j,\mathrm{K}^*}=f_{\mathrm{K}^*},\quad \forall\ \mathrm{K}^*\in\mathfrak{M}_j^*, \tag{5}$$

$$-\sum_{\mathrm{D}\in\mathfrak{D}_{\mathrm{K}^*}}\frac{m_{\sigma^*}}{m_{\mathrm{K}^*}}\left(A_{\mathrm{D}}\nabla^{\mathrm{D}}u_{\mathcal{T}_j},\mathbf{n}_{\sigma^*\mathrm{K}^*}\right)-\frac{m_{\sigma_{\mathrm{K}^*}}}{m_{\mathrm{K}^*}}\psi_{j,\mathrm{K}^*}+\eta_{\mathrm{K}^*}u_{j,\mathrm{K}^*}=f_{\mathrm{K}^*},\forall\mathrm{K}^*\in\partial\mathfrak{M}^*_{\Gamma_j}, \tag{6}$$

$$\left(A_{\mathrm{D}}\nabla^{\mathrm{D}}u_{\mathcal{T}_j},\mathbf{n}_{\sigma\mathrm{L}}\right)+\Lambda_{\mathrm{L}}^{\partial\mathfrak{M}_{\Gamma_j}}(u_{\partial\mathfrak{M}_{\Gamma_j}})=h_{j,\mathrm{L}},\quad \forall\ \mathrm{L}\in\partial\mathfrak{M}_{\Gamma_j}, \tag{7}$$

$$\psi_{j,\mathrm{K}^*}+\Lambda_{\mathrm{K}^*}^{\partial\mathfrak{M}^*_{\Gamma_j}}(u_{\partial\mathfrak{M}^*_{\Gamma_j}})=h_{j,\mathrm{K}^*},\quad \forall\ \mathrm{K}^*\in\partial\mathfrak{M}^*_{\Gamma_j}, \tag{8}$$

$$u_{j,\mathrm{K}}=0,\quad \forall\ \mathrm{K}\in\partial\mathfrak{M}_j\cap\partial\Omega,\qquad u_{j,\mathrm{K}^*}=0,\quad \forall\ \mathrm{K}^*\in\partial\mathfrak{M}_j^*\cap\partial\Omega, \tag{9}$$

The transmission operators $\Lambda^{\partial\mathfrak{M}_{\Gamma_j}}$ and $\Lambda^{\partial\mathfrak{M}^*_{\Gamma_j}}$ are defined by

$$\Lambda_{\mathrm{L}_s}^{\partial\mathfrak{M}_{\Gamma_j}}(u_{\partial\mathfrak{M}_{\Gamma_j}}) := pu_{j,\mathrm{L}_s} - A_{yy}\frac{q}{m_{\sigma_s}}\left(\frac{u_{j,\mathrm{L}_{s+1}}-u_{j,\mathrm{L}_s}}{m_{\sigma_{\mathrm{K}^*_{s+1}}}}-\frac{u_{j,\mathrm{L}_s}-u_{j,\mathrm{L}_{s-1}}}{m_{\sigma_{\mathrm{K}^*_s}}}\right),$$

for $s=1,\cdots,N_j$, with $u_{j,\mathrm{L}_0}=u_{j,\mathrm{L}_{N_j+1}}=0$, and for $s=2,\cdots,N_j$ by

$$\Lambda_{\mathrm{K}^*_s}^{\partial\mathfrak{M}^*_{\Gamma_j}}(u_{\partial\mathfrak{M}^*_{\Gamma_j}}) := pu_{j,\mathrm{K}^*_s} - A_{yy}\frac{q}{m_{\sigma_{\mathrm{K}^*}s}}\left(\frac{u_{j,\mathrm{K}^*_{s+1}}-u_{j,\mathrm{K}^*_s}}{m_{\sigma_s}}-\frac{u_{j,\mathrm{K}^*_s}-u_{j,\mathrm{K}^*_{s-1}}}{m_{\sigma_{s-1}}}\right).$$

Note that the edges $\sigma_1,\ldots,\sigma_{N_j}$ have been sorted such that $\sigma_s\cap\sigma_{s+1}\neq\emptyset$, and $x_{\mathrm{K}^*_s},x_{\mathrm{K}^*_{s+1}}$ are the vertices of σ_s, where $x_{\mathrm{K}^*_s}=\sigma_s\cap\sigma_{s-1}$. Note also that $u_{j,\mathrm{K}^*_1}=u_{j,\mathrm{K}^*_{N_j+1}}=0$ because of the homogeneous boundary condition on $\partial\Omega$. Equations (4)-(6) correspond to approximations of the equation after integration on $\mathfrak{M}_j$, $\mathfrak{M}_j^*$ and $\partial\mathfrak{M}_j^*$; equations (7) and (8) stem from the transmission condition on $\partial\mathfrak{M}_{\Gamma_j}$ and $\partial\mathfrak{M}^*_{\Gamma_j}$; equation (9) corresponds to the Dirichlet boundary condition on $\partial\Omega$. One can show that this discrete formulation is well posed, see [6, Theorem 3.1].

DDFV Schwarz algorithm. The DDFV optimized Schwarz algorithm performs for an arbitrary initial guess $h^0_{\mathcal{T}_j}\in\mathbb{R}^{\partial\mathfrak{M}_{\Gamma_j}\cup\partial\mathfrak{M}^*_{\Gamma_j}}$, $(j,i)=(1,2)$ or $(j,i)=(2,1)$ and $l=1,2,\ldots$ the following steps:

- Compute the solutions $u^{l+1}_{\mathcal{T}_j}\in\mathbb{R}^{\mathcal{T}_j}$ of $\mathcal{L}^{\mathcal{T}_j}_{\Omega_j}(u^{l+1}_{\mathcal{T}_j},f_{\mathcal{T}_j},h^l_{\mathcal{T}_j})=0$.

- Then, we define $P_{\partial\mathfrak{M}^*_{\Gamma_j}}(u^{l+1}_{\mathcal{T}_i})$ on the vertices of the interface Γ_j as follows: for $x_{\mathrm{K}^*_j} \in \partial\mathfrak{M}^*_{\Gamma_j}$, there exists a unique vertex $x_{\mathrm{K}^*} \in \mathfrak{M}^*_i$ such that $x_{\mathrm{K}^*_j} = x_{\mathrm{K}^*}$, we set $u^{l+1}_{\mathrm{K}^*_j} = u^{l+1}_{\mathrm{K}^*}$.
- Then, we define $P_{\partial\mathfrak{M}_{\Gamma_j}}(u^{l+1}_{\mathcal{T}_i})$ on the interface Γ_j as follows. For $\mathrm{D} \in \mathfrak{D}_{\Gamma_j}$, there exist two half-diamonds D_i and D_j such that $\mathrm{D} = \mathrm{D}_i \cup \mathrm{D}_j$. We define $P_\sigma(u^{l+1}_{\mathcal{T}_i}) = u_{\mathrm{L}}$ such that

$$\left(A_{\mathrm{D}_i}\nabla^{\mathrm{D}_i} u^{l+1}_{\mathcal{T}_i}, \mathbf{n}_{\sigma\mathrm{L}_i}\right) = \left(A_{\mathrm{D}_j}\nabla^{\mathrm{D}_j} u^{l+1}_{\mathcal{T}_j}, \mathbf{n}_{\sigma\mathrm{L}_j}\right).$$

- We evaluate the flux unknowns. For $x_{\mathrm{K}^*_j} \in \partial\mathfrak{M}^*_{\Gamma_j}$, there exists a unique vertex $x_{\mathrm{K}^*} \in \mathfrak{M}^*_i$ such that $x_{\mathrm{K}^*_j} = x_{\mathrm{K}^*}$. We set $\mathrm{K}^*_i = \mathrm{K}^* \cap (\Omega_i \setminus \Omega_j)$

$$\frac{m_{\sigma_{\mathrm{K}^*}}}{m_{\mathrm{K}^*_i}}\psi^{l+1}_{i,\mathrm{K}^*} = -\sum_{\mathrm{D}\in\mathfrak{D}_{\mathrm{K}^*_i}} \frac{m_{\sigma^*}}{m_{\mathrm{K}^*_i}} \left(A_{\mathrm{D}}\nabla^{\mathrm{D}} u^{l+1}_{\mathcal{T}_i}, \mathbf{n}_{\sigma^*\mathrm{K}^*_i}\right) + \eta_{\mathrm{K}^*} u^{l+1}_{i,\mathrm{K}^*_i} - f_{\mathrm{K}^*_i}.$$

- We evaluate the new interface values $h^{l+1}_{\mathcal{T}_j}$ by

$$h^{l+1}_{j,\mathrm{L}} = -\left(A_{\mathrm{D}}\nabla^{\mathrm{D}} u^{l+1}_{\mathcal{T}_i}, \mathbf{n}_{\sigma\mathrm{L}_i}\right) + \Lambda_{\mathrm{L}}^{\partial\mathfrak{M}_{\Gamma_j}}(P_{\partial\mathfrak{M}_{\Gamma_j}}(u^{l+1}_{\mathcal{T}_i})),\ \forall \mathrm{L} \in \partial\mathfrak{M}_{\Gamma_j}, \quad (10a)$$

$$h^{l+1}_{j,\mathrm{K}^*} = -\psi^{l+1}_{i,\mathrm{K}^*} + \Lambda_{\mathrm{K}^*}^{\partial\mathfrak{M}^*_{j,\Gamma}}(P_{\partial\mathfrak{M}^*_{\Gamma_j}}(u^{l+1}_{\mathcal{T}_i})),\ \forall \mathrm{K}^* \in \partial\mathfrak{M}^*_{\Gamma_j}. \quad (10b)$$

4 Convergence factors

We now give the convergence factors of the DDFV Schwarz algorithm for a rectangular two subdomain decomposition, $\Omega := (-a_1, a_2) \times (0, b)$, $\Omega_1 := (-a_1, L) \times (0, b)$ and $\Omega_2 := (0, a_2) \times (0, b)$, $L \geq 0$ being the overlap size.

Continuous case. The error $e^n_j := u - u^n_j$ satisfies homogeneous Dirichlet boundary conditions, and can thus be expanded in a Fourier sine series, $e^n_j(x, y) = \sum_{k\in E} \hat{e}^n_j(x, k) \sin ky$ with the set $E := \frac{\pi\mathbb{N}^+}{b}$. A direct computation with

$$r(k) := \frac{\sqrt{\eta A_{xx} + k^2 \det A}}{A_{xx}} \quad (11)$$

leads to the continuous convergence factors for classical and optimized Schwarz:

$$\rho^{cla}_{c,a} = \frac{\sinh(r(a_2 - L))}{\sinh(r(L + a_1))}\frac{\sinh(ra_1)}{\sinh(ra_2)}, \quad (12)$$

$$\rho_{c,a} = \rho^{cla}_{c,a}\frac{P - A_{xx}r\coth((a_2 - L)r)}{P + A_{xx}r\coth((a_1 + L)r)}\frac{P - A_{xx}r\coth(a_1 r)}{P + A_{xx}r\coth(a_2 r)}. \quad (13)$$

Discrete case on a Cartesian mesh. Let the mesh sizes be (h_x, h_y), and $M_j = N_j h_x$, $L = M h_x$. When $A_{xy} = 0$, the equations for the primal and dual unknowns decouple into two finite difference schemes of order 2: the primal unknowns are solutions of a cell-centered (CC) scheme, and the dual unknowns are solutions of a vertex centered (VC) scheme. Using again Fourier analysis, with the notation

$$\begin{aligned} &\alpha(k) := \tfrac{4A_{yy}}{{h_y}^2}\sin^2(\tfrac{kh_y}{2}), \quad \mu(k) := \tfrac{h_x^2}{A_{xx}}(\alpha(k)+\eta), \\ &\lambda(k) := 1 + \tfrac{\mu(k)}{2} - \sqrt{\mu(k) + \tfrac{\mu(k)^2}{4}} \in (0,1),\ \tilde{r}(k) := -\ln\lambda(k) > 0, \end{aligned} \tag{14}$$

the discrete convergence factor for classical Schwarz for both CC and VC is

$$\rho_{d,M}^{cla} = \frac{\sinh((M_2 - M)\tilde{r})}{\sinh((M_1 + M)\tilde{r})}\frac{\sinh(M_1\tilde{r})}{\sinh(M_2\tilde{r})}. \tag{15}$$

For optimized Schwarz, with $P(k) := p + q\alpha(k)$, we get for VC and CC

$$\begin{aligned} \rho_{dvc,M} &= \rho_{d,M}^{cla}\frac{P - \frac{A_{xx}}{h_x}\sinh\tilde{r}\coth((M_2-M)\tilde{r})}{P + \frac{A_{xx}}{h_x}\sinh\tilde{r}\coth((M_1+M)\tilde{r})}\frac{P - \frac{A_{xx}}{h_x}\sinh\tilde{r}\coth(M_1\tilde{r})}{P + \frac{A_{xx}}{h_x}\sinh\tilde{r}\coth(M_2\tilde{r})}, \\ \rho_{dcc,M} &= \rho_{d,M}^{cla}\frac{P - 2\frac{A_{xx}}{h_x}\tanh\frac{\tilde{r}}{2}\coth((M_2-M)\tilde{r})}{P + 2\frac{A_{xx}}{h_x}\tanh\frac{\tilde{r}}{2}\coth((M_1+M)\tilde{r})}\frac{P - 2\frac{A_{xx}}{h_x}\tanh\frac{\tilde{r}}{2}\coth(M_1\tilde{r})}{P + 2\frac{A_{xx}}{h_x}\tanh\frac{\tilde{r}}{2}\coth(M_2\tilde{r})}. \end{aligned} \tag{16}$$

We also obtain the classical unbounded domain convergence factors $\rho_{c,\infty}^{cla}$, $\rho_{c,\infty}$, $\rho_{d,\infty}^{cla}$ $\rho_{dvc,\infty}$, and $\rho_{dcc,\infty}$ from the bounded ones in (12), (13), (15) and (16) by passing to the limit as a_1, a_2 and M_1, M_2 go to infinity, which greatly simplifies the expressions, see [5, Section 5] for the continuous case. Since the convergence speed of the methods is bounded by the largest contraction factor over all k, we further introduce the corresponding upper case quantity $R := \sup_{k\in E}|\rho|$, and add a superscript R^*, p^* and q^* to denote the quantities obtained when R has been minimized using p and q.

5 Importance of a Bounded Domain Discrete Analysis

For isotropic diffusion, bounded and unbounded domain analyses both at the continuous and discrete level give very similar optimized parameters (p^*, q^*) as in the non-overlapping case [6]. We show now that for anisotropic diffusion the discrete bounded domain analysis gives much more accurate predictions $(p^*_{dvc,M}, q^*_{dvc,M})$, and $(p^*_{dcc,M}, q^*_{dcc,M})$. We choose $A_{xx} = 16$, $A_{yy} = 1$ and $A_{xy} = 0$, and decompose the domain $\Omega := (-1,1)\times(0,1)$ into two subdomains $\Omega_1 := (-1, L)\times(0,1)$ and $\Omega_2 := (0,1)\times(0,1)$. We choose for the mesh sizes $h_x = h_y = h$ and for the overlap $L = h$. We also compute the numerically best working transmission parameters $(p^*_{dvc,num}, q^*_{dvc,num})$, and $(p^*_{dcc,num}, q^*_{dcc,num})$ by minimizing the numerical error remaining after $n = 50$

	Theoretical and best numerical parameters									
h	$p^*_{c,\infty}$	$p^*_{c,a}$	$p^*_{dvc,\infty}$	$p^*_{dvc,M}$	$p^*_{vc,num}$	$q^*_{c,\infty}$	$q^*_{c,a}$	$q^*_{dvc,\infty}$	$q^*_{dvc,M}$	$q^*_{vc,num}$
2^{-3}	13.3040	20.6673	12.1818	19.7453	19.7200	0.2137	0.1661	0.2623	0.1995	0.1997
2^{-4}	15.8876	22.9419	14.7928	21.5210	21.4130	0.1391	0.1132	0.1688	0.1393	0.1395
2^{-5}	18.4998	26.0734	17.5707	24.6458	24.5234	0.0936	0.0769	0.1089	0.0921	0.0926
2^{-6}	21.2112	29.6330	20.6142	28.4895	28.2013	0.0647	0.0531	0.0707	0.0602	0.0604

	Theoretical convergence factors				Numerically measured convergence factors				
h	$R^*_{c,\infty}$	$R^*_{c,a}$	$R^*_{dvc,\infty}$	$R^*_{dvc,M}$	$R_{c,\infty}$	$R_{c,a}$	$R_{dvc,\infty}$	$R_{dvc,M}$	$R^*_{vc,num}$
2^{-3}	0.0049	0.0012	0.0027	0.0003	0.0154	0.0013	0.0205	0.0003	0.0003
2^{-4}	0.0161	0.0079	0.0111	0.0043	0.0183	0.0079	0.0138	0.0042	0.0041
2^{-5}	0.0347	0.0223	0.0280	0.0159	0.0338	0.0222	0.0274	0.0159	0.0156
2^{-6}	0.0596	0.0440	0.0541	0.0371	0.0561	0.0439	0.0526	0.0370	0.0360

Table 1 $A_{xx} = 16, A_{yy} = 1$, Ventcell coefficients, Vertex Centered (VC)

alternating Schwarz iterations with random initial guess solving directly the homogeneous error equations, and the corresponding numerical convergence factor $R^*_{num} := (||e^n||/||e^1||)^{\frac{1}{n-1}}$ where $||e^n||$ denotes the L^2 norm of the error e^n on the interface of the subdomains. We see in Table 1 in the top part that for VC the optimized parameters (p^*, q^*) are quite different for the bounded and unbounded analysis, and there is also a difference between discrete and continuous analysis. The asymptotic growth rate is however the same for all different analysis types, just the constant differs. The theoretically optimized convergence factors R^* in the bottom part of Table 1 on the left, and the numerically measured convergence factors R using the theoretically optimized parameters in the bottom part of Table 1 on the right clearly show that the best results are obtained for the discrete bounded domain analysis technique, very close to the numerically optimized $R^*_{vc,num}$. The results in Table 2 for CC are similar, only the q^* are a bit smaller, and convergence is slightly slower for CC than for VC. Table 3 shows the results for DDFV which computes both VC and CC interlaced simultaneously. We see that both the optimized

	Theoretical and best numerical parameters									
h	$p^*_{c,\infty}$	$p^*_{c,a}$	$p^*_{dcc,\infty}$	$p^*_{dcc,M}$	$p^*_{cc,num}$	$q^*_{c,\infty}$	$q^*_{c,a}$	$q^*_{dcc,\infty}$	$q^*_{dcc,M}$	$q^*_{cc,num}$
2^{-3}	13.6259	21.0138	12.4676	19.9705	19.9264	0.2015	0.1568	0.2441	0.1837	0.1840
2^{-4}	16.0014	23.1167	15.0389	21.8064	21.7329	0.1363	0.1105	0.1601	0.1315	0.1316
2^{-5}	18.5257	26.1345	17.8211	24.9634	24.8306	0.0932	0.0763	0.1041	0.0878	0.0882
2^{-6}	21.2157	29.6388	20.8856	28.5642	28.5642	0.0648	0.0531	0.0678	0.0577	0.0579

	Theoretical convergence factors				Numerically measured convergence factors				
h	$R^*_{c,\infty}$	$R^*_{c,a}$	$R^*_{dcc,\infty}$	$R^*_{dcc,M}$	$R_{c,\infty}$	$R_{c,a}$	$R_{dcc,\infty}$	$R_{dcc,M}$	$R^*_{cc,num}$
2^{-3}	0.0058	0.0016	0.0032	0.0005	0.0137	0.0017	0.0193	0.0005	0.0005
2^{-4}	0.0167	0.0084	0.0121	0.0049	0.0182	0.0084	0.0141	0.0049	0.0048
2^{-5}	0.0349	0.0226	0.0297	0.0172	0.0338	0.0226	0.0293	0.0172	0.0169
2^{-6}	0.0596	0.0440	0.0566	0.0392	0.0563	0.0439	0.0549	0.0391	0.0381

Table 2 $A_{xx} = 16, A_{yy} = 1$, Ventcell coefficients, Cell Centered (CC)

h	$p^*_{dvc,M}$	$q^*_{dvc,M}$	$R_{ddfv,num}$	$p^*_{dcc,M}$	$q^*_{dcc,M}$	$R_{ddfv,num}$	$p^*_{ddfv,num}$	$q^*_{ddfv,num}$	$R^*_{ddfv,num}$
2^{-3}	19.7453	0.1995	0.0369	19.9705	0.1837	0.0314	20.6898	0.1836	0.0242
2^{-4}	21.50210	0.1393	0.0780	21.8064	0.1315	0.0713	22.1314	0.1324	0.0676
2^{-5}	24.64583	0.0921	0.1326	24.8306	0.0878	0.1278	24.8414	0.0891	0.1258
2^{-6}	28.4895	0.0602	0.1906	28.5642	0.0577	0.1909	28.2904	0.0593	0.1881

Table 3 $A_{xx} = 16, A_{yy} = 1$, DDFV with VC and CC coefficients from the discrete bounded domain analysis, and best working ones for DDFV

parameters from the VC and CC discrete and bounded domain analysis give very good performance, the CC ones just being a little better.

To conclude, we presented a first step for the design and analysis of optimized overlapping DDFV Schwarz methods for anisotropic diffusion. Using the fact that for rectangular meshes the primal and dual unknowns decouple, we computed two convergence factors, whose maximum represents an upper bound on the convergence of the DDFV Schwarz method. Our analysis will allow us to study anisotropic meshes, and we will also investigate the influence of non-matching meshes in the different subdomains. Finally, a theoretical optimization of the coupled convergence factors in the parameters is needed to get closed formulas for the optimized parameters.

References

[1] Boyer, F., Hubert, F.: Finite volume method for 2D linear and nonlinear elliptic problems with discontinuities. SIAM J. Numer. Anal. **46** (2008)
[2] Boyer, F., Hubert, F., Krell, S.: Non-overlapping Schwarz algorithm for solving 2D m-DDFV schemes. IMA Jour. Num. Anal. **30** (2009)
[3] Domelevo, K., Omnes, P.: A finite volume method for the Laplace equation on almost arbitrary two-dimensional grids. M2AN Math. Model. Numer. Anal. **39**(6), 1203–1249 (2005)
[4] Gander, M.J.: Optimized Schwarz method. SIAM Journal on Numerical Analysis **44**(2), 699–731 (2006)
[5] Gander, M.J., Dubois, O.: Optimized Schwarz methods for a diffusion problem with discontinuous coefficient. Numerical Algorithms **69**(1), 109–144 (2015)
[6] Gander, M.J., Halpern, L., Hubert, F., Krell, S.: Optimized Schwarz Methods for Anisotropic Diffusion with Discrete Duality Finite Volume Discretizations (2018). URL `https://hal.archives-ouvertes.fr/hal-01782357`. Submitted
[7] Hermeline, F.: Approximation of diffusion operators with discontinuous tensor coefficients on distorted meshes. Comput. Methods Appl. Mech. Engrg. **192**(16-18), 1939–1959 (2003)